

SIMULATION IN PRIMITIVE VARIABLES OF INCOMPRESSIBLE FLOW WITH PRESSURE NEUMANN CONDITION

JULIO R. CLAEYSSEN^{a,*}, RODRIGO B. PLATTE^{a,1} AND ELBA BRAVO^{b,2}

^a *Universidade Federal do Rio Grande do Sul, Instituto de Matematica-PROMEC-CESUP, PO Box 10673, 90.001-000 Porto Alegre, RS, Brazil*

^b *Universidade Regional Integrada-URI, Departamento de Engenharia e Ciencias da Computação, 98.400-000 Frederico Westphalen, RS, Brazil*

SUMMARY

A velocity–pressure algorithm, in primitive variables and finite differences, is developed for incompressible viscous flow with a Neumann pressure boundary condition. The pressure field is initialized by least-squares and updated from the Poisson equation in a direct weighted manner. Simulations with the cavity problem were made for several Reynolds numbers. The expected displacement of the central vortex was obtained, as well as the development of secondary and tertiary eddies. Copyright © 1999 John Wiley & Sons, Ltd.

KEY WORDS: incompressible flow; primitive variables; velocity–pressure algorithm

1. INTRODUCTION

A velocity–pressure algorithm for incompressible viscous flow is developed in primitive variables by using finite differences, a Neumann boundary condition for the pressure and without any iteration method for updating the pressure.

The incorporation of the Neumann condition for incompressible flow has been discussed in detail in a remarkable work by Gresho and Sani [1]. From a mathematical point of view, the system of equations governing an incompressible flow is singular with respect to the pressure. There is no evolutive equation for the pressure. In practice, the system is usually considered as the momentum equation subject to a solenoidal restriction for the velocity field. The initial and boundary conditions are being prescribed only for the velocity field.

The discretization by difference methods of the Navier–Stokes equations on a staggered grid [23], when formulated in matrix terms, allows the identification of a singular evolutive matrix system. When the Poisson equation for the pressure is derived and its integration performed, it can be observed that a clear influence of the Neumann condition arises. From this, a non-singular system for determining the pressure values at the interior points can be extracted. The initialization process of the pressure, by a least-squares procedure, somehow incorporates

* Correspondence to: Universidade Federal do Rio Grande do Sul, Instituto de Matematica-PROMEC-CESUP, PO Box 10673, 90.001-000 Porto Alegre, RS, Brazil. E-mail: julio@mat.ufrgs.br

¹ E-mail: rbplatte@mat.ufrgs.br

² E-mail: eoba@inf.uri.br

an optimal pressure as a starting point, instead of employing an arbitrary constant as it usually does with iterative methods. The values of the velocity and pressure at interior points can be well-determined by the forward Euler method for the velocity and by solving a non-singular Poisson equation without iteration. The latter means that the values of the pressure and velocity are incorporated as soon as they are computed.

The formulation of the present algorithm follows the unified operator approach introduced by Casulli [2,20], which allows the consideration of, with minor modifications, the upwind and semi-Lagrangean methods.

This velocity–pressure algorithm with central differences has been tested with the cavity flow problem for a wide range of Reynolds numbers. The displacement of the central vortex to the geometrical center of the cavity was obtained when increasing the Reynolds number, as earlier established by Burggraf [3], Ghia *et al.* [4] and Schreiber and Keller [5] among others; also the development of secondary and tertiary vortices.

2. THE CONTINUUM EQUATIONS FOR INCOMPRESSIBLE FLOW

In this section a brief account of the prescription of the Neumann condition is given, as performed by Gresho and Sani [1]. The Navier–Stokes equations for the velocity $\mathbf{u}(\mathbf{x}, t)$ and pressure $p(\mathbf{x}, t)$ with initial and boundary conditions for the velocity, constitute the system

$$\frac{\partial \mathbf{u}}{\partial t} + \mathbf{u} \cdot \nabla \mathbf{u} + \nabla p = \nu \nabla^2 \mathbf{u}, \quad t > 0, \quad (1)$$

$$\nabla \cdot \mathbf{u} = 0, \quad (2)$$

$$\mathbf{u}(\mathbf{x}, 0) = \mathbf{u}_0(\mathbf{x}), \quad \mathbf{x} \text{ in } \bar{\Omega} = \Omega \oplus \Gamma, \quad (3)$$

$$\mathbf{u} = \mathbf{w}(\mathbf{x}, t) \quad \text{in } \Gamma = \partial\Omega. \quad (4)$$

Here Ω denotes a limited two-dimensional region, with Γ as its boundary, and

$$\nabla \cdot \mathbf{u}_0 = 0 \quad \text{in } \Omega \quad (5)$$

is an initial solenoidal velocity field. From the above system, the initial normal velocity follows as

$$\mathbf{u}_0 \cdot \mathbf{n} = \mathbf{w}(\mathbf{x}, 0) \cdot \mathbf{n} \quad \text{on } \Gamma, \quad (6)$$

and the global mass conservation as

$$\int_{\Gamma} \mathbf{u} \cdot \mathbf{n} \, dx = 0. \quad (7)$$

It is observed that no initial nor boundary conditions are prescribed for the pressure. Thus, p is determined up to an additive constant corresponding to the level of hydrostatic pressure.

The conditions of an initial velocity field solenoidal and normal velocity compatible with the above boundary conditions are required for the problem to have a well-defined, unique and solenoidal solution for all $t \geq 0$ [6]. The initial tangential velocity field is not required to be compatible with the boundary conditions. If so, then the solution may be smoother [1].

By assuming adequate differentiability hypotheses, the Poisson equation can be derived by taking the divergence of the momentum equation and using the vector identity

$$\nabla^2 \mathbf{u} = \nabla(\nabla \cdot \mathbf{u}) - \nabla \times \nabla \times \mathbf{u}. \quad (8)$$

Therefore,

$$\nabla \cdot (\mathbf{u} \cdot \nabla \mathbf{u}) + \nabla^2 p = \left(\nu \nabla^2 \Theta - \frac{\partial \Theta}{\partial t} \right) \quad \text{in } \Omega, \tag{9}$$

where $\Theta = \nabla \cdot \mathbf{u}$.

Since the prescribed conditions for \mathbf{u} in Γ are valid everywhere in time, i.e.

$$\nabla \cdot \mathbf{u} = 0 \quad \text{in } \bar{\Omega} \text{ for } t \geq 0, \tag{10}$$

they can be substituted into the equation for Θ and the Poisson equation for the pressure can be obtained

$$\nabla^2 p = -\nabla \cdot (\mathbf{u} \cdot \nabla \mathbf{u}) \quad \text{in } \Omega \text{ for } t \geq 0. \tag{11}$$

Consider the equivalent equation

$$\nabla^2 p = \nabla \cdot (\nu \nabla^2 \mathbf{u} - \mathbf{u} \cdot \nabla \mathbf{u}). \tag{12}$$

In order to complete the specification of the problem for the pressure, boundary conditions should be imposed for the pressure on Γ . Since the last two equations have been derived, the boundary conditions should be also derived. One obvious manner is to set the momentum equation as valid on the boundary. However, this is a vector equation and only one scalar boundary condition is required. Either the normal or the tangential projection of the momentum equation upon Γ can be chosen. The first option gives

$$\mathbf{n} \cdot \nabla p = \frac{\partial p}{\partial n} = \nu \nabla^2 u_n - \left(\frac{\partial u_n}{\partial t} + \mathbf{u} \cdot \nabla u_n \right) \quad \text{in } \Gamma \text{ for } t \geq 0. \tag{13}$$

Thus, Equations (11), (12) and (13) constitute a Neumann problem for the pressure.

On the other hand, the tangential component of the momentum equation upon Γ gives a Dirichlet condition of type

$$\tau \cdot \nabla p = \frac{\partial p}{\partial \tau} = \nu \nabla^2 u_\tau - \left(\frac{\partial u_\tau}{\partial t} + \mathbf{u} \cdot \nabla u_\tau \right), \tag{14}$$

where the value of p on Γ , i.e. Dirichlet data, is provided for by integration of (14) through τ .

The determination of the solution of the Poisson equation (11) with Neumann boundary conditions (13) requires holding the compatibility relationship

$$\iint_{\Omega} \nabla^2 p \, d\Omega = \iint_{\Omega} -\nabla \cdot (\mathbf{u} \cdot \nabla \mathbf{u}) \, d\Omega = \oint_{\Gamma} p_n \, d\Gamma, \tag{15}$$

where $p_n = \mathbf{n} \cdot \nabla p$ and \mathbf{n} is an exterior normal unit vector to Γ .

3. DISCRETIZATION OF THE NAVIER–STOKES EQUATIONS

For a non-dimensioned two-dimensional incompressible viscous flow, the primitive equations are

$$\frac{\partial u}{\partial t} + u \frac{\partial u}{\partial x} + v \frac{\partial u}{\partial y} = -\frac{\partial p}{\partial x} + \frac{1}{Re} \left(\frac{\partial^2 u}{\partial x^2} + \frac{\partial^2 u}{\partial y^2} \right), \tag{16}$$

$$\frac{\partial v}{\partial t} + u \frac{\partial v}{\partial x} + v \frac{\partial v}{\partial y} = -\frac{\partial p}{\partial y} + \frac{1}{Re} \left(\frac{\partial^2 v}{\partial x^2} + \frac{\partial^2 v}{\partial y^2} \right), \quad (17)$$

$$\frac{\partial u}{\partial x} + \frac{\partial v}{\partial y} = 0, \quad (18)$$

where $u(x, y, t)$ and $v(x, y, t)$ denote the velocity components in the x - and y -directions, $p(x, y, t)$ the pressure and $Re \geq 0$ the Reynolds number respectively. This system can be written in the operator compact form

$$M \frac{\partial U}{\partial t} + NU = -PU + LU, \quad (19)$$

where

$$U = \begin{bmatrix} u \\ v \\ p \end{bmatrix}, \quad M = \begin{bmatrix} 1 & 0 & 0 \\ 0 & 1 & 0 \\ 0 & 0 & 0 \end{bmatrix},$$

$$N = \begin{bmatrix} \left(u \frac{\partial}{\partial x} + v \frac{\partial}{\partial y} \right) & 0 & 0 \\ 0 & \left(u \frac{\partial}{\partial x} + v \frac{\partial}{\partial y} \right) & 0 \\ 0 & 0 & 0 \end{bmatrix}, \quad P = \begin{bmatrix} 0 & 0 & \frac{\partial}{\partial x} \\ 0 & 0 & \frac{\partial}{\partial y} \\ 0 & 0 & 0 \end{bmatrix},$$

$$L = \begin{bmatrix} \frac{1}{Re} \left(\frac{\partial^2}{\partial x^2} + \frac{\partial^2}{\partial y^2} \right) & 0 & 0 \\ 0 & \frac{1}{Re} \left(\frac{\partial^2}{\partial x^2} + \frac{\partial^2}{\partial y^2} \right) & 0 \\ \frac{\partial}{\partial x} & \frac{\partial}{\partial y} & 0 \end{bmatrix}.$$

Central differences will now be used for approximating the spatial derivatives. For simplicity, the formulation will be restricted to a rectangular staggered grid (Figure 1).

Setting $\Delta x_i = \Delta x$, $i = 0, \dots, n$ and $\Delta y_j = \Delta y$, $j = 0, \dots, m$, let

$$u_{i,j} = u(i\Delta x, (j + \frac{1}{2})\Delta y),$$

$$v_{i,j} = v((i + \frac{1}{2})\Delta x, j\Delta y),$$

$$p_{i,j} = p((i + \frac{1}{2})\Delta x, (j + \frac{1}{2})\Delta y),$$

write Equations (16) and (17) as

$$\frac{\partial u}{\partial t} = F_1(u, v) - G_1(p), \quad (20)$$

$$\frac{\partial v}{\partial t} = F_2(u, v) - G_2(p) \quad (21)$$

respectively, then apply spatial central differences. It turns out that

$$F_1(u, v) = -u_{i,j} \frac{u_{i+1,j} - u_{i-1,j}}{2\Delta x} - v|_{u_{i,j}} \frac{u_{i,j+1} - u_{i,j-1}}{2\Delta y} + \frac{1}{Re} \left(\frac{u_{i+1,j} - 2u_{i,j} + u_{i-1,j}}{\Delta x^2} + \frac{u_{i,j+1} - 2u_{i,j} + u_{i,j-1}}{\Delta y^2} \right), \tag{22}$$

$$F_2(u, v) = -u|_{v_{i,j}} \frac{v_{i+1,j} - v_{i-1,j}}{2\Delta x} - v_{i,j} \frac{v_{i,j+1} - v_{i,j-1}}{2\Delta y} + \frac{1}{Re} \left(\frac{v_{i+1,j} - 2v_{i,j} + v_{i-1,j}}{\Delta x^2} + \frac{v_{i,j+1} - 2v_{i,j} + v_{i,j-1}}{\Delta y^2} \right). \tag{23}$$

Similarly,

$$G_1(p) = \frac{p_{i,j} - p_{i-1,j}}{\Delta x}, \tag{24}$$

$$G_2(p) = \frac{p_{i,j} - p_{i,j-1}}{\Delta y}. \tag{25}$$

Here $v|_{u_{i,j}}$ and $u|_{v_{i,j}}$ denote the average values

$$v|_{u_{i,j}} = \frac{v_{i,j+1} + v_{i,j} + v_{i+1,j+1} + v_{i+1,j-1}}{4} \tag{26}$$

and

$$u|_{v_{i,j}} = \frac{u_{i,j+1} + u_{i,j} + u_{i+1,j+1} + u_{i+1,j-1}}{4}. \tag{27}$$

3.1. Matrix formulation

The above spatial discretization procedure, together with the pressure Neumann condition, for the Navier–Stokes equations on a rectangular staggered grid amounts, in matrix terms, to replace (19) by the spatial approximation [17]

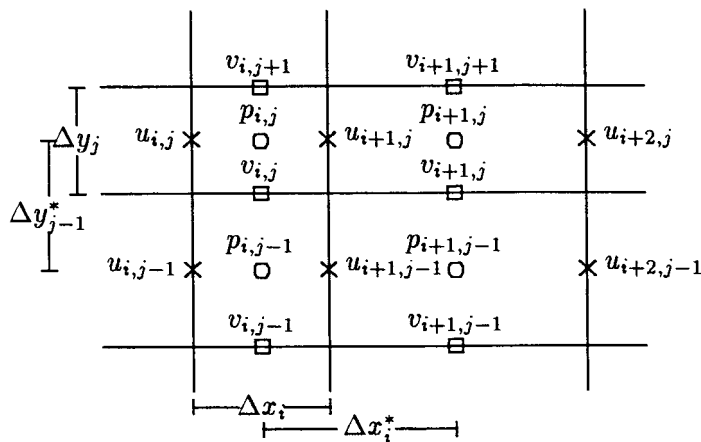


Figure 1. Staggered grid.

$$\mathbb{M} \frac{d\mathbb{U}}{dt} + \mathbb{N}(\mathbb{U})\mathbb{U} + \mathbb{N}^F(\mathbb{U}, \mathbb{U}^F)\mathbb{U}^F = -\mathbb{P}\mathbb{U} - \mathbb{P}^F(\mathbb{U}, \mathbb{U}^F) + \mathbb{L}\mathbb{U} + \mathbb{L}^F\mathbb{U}^F. \quad (28)$$

Here $\mathbb{U} = [U_{i,j}]$, where $U_{i,j}$ includes the values $u_{i+1/2,j}$, $v_{i,j+1/2}$, $p_{i,j}$ at a cell (i, j) . The vector \mathbb{U}^F corresponds to the boundary values of u , v and p . The matrices \mathbb{M} , \mathbb{N} , \mathbb{L} , \mathbb{P} are the corresponding spatial approximation of the continuous terms and \mathbb{N}^F , \mathbb{L}^F , \mathbb{P}^F are matrices that contain boundary values. The above systems are singular once \mathbb{M} is a singular matrix [18].

If an upwind approximation is used for the velocity field and central differences are kept for the pressure gradient, it will turn out that the matrix formulation reads [19],

$$\mathbb{M} \frac{d\mathbb{U}}{dt} + \mathbb{N}(\mathbb{U}, \mathbb{U}^F)\mathbb{U} + \mathbb{N}^F(\mathbb{U}, \mathbb{U}^F)\mathbb{U}^F = -\mathbb{P}\mathbb{U} - \mathbb{P}^F(\mathbb{U}, \mathbb{U}^F) + \mathbb{L}\mathbb{U} + \mathbb{L}^F\mathbb{U}^F. \quad (29)$$

From such equations, it is observed that although the \mathbb{N} matrix is different for each method, there is a direct influence of boundary values on the non-linear convection matrix when discretized by the upwind method. This is not the case for central differences, and in numerical terms it means that boundary values do not interfere with the numerical convection at interior points.

The above matrix formulation will be of a similar nature for non-rectangular domains.

3.2. Time discretization

The time discretization of the momentum equations, besides modifying the order of approximation, raises numerical stability problems. Although implicit methods have better stability properties, they are expensive to implement. In this paper, the explicit Euler or Adams–Bashforth methods will be used.

The Adams–Bashforth method, applied to Equations (20) and (21), can be written as

$$u^{k+1} = u^k + \Delta t \sum_{l=0}^{n_p-1} \alpha_l [F_1(u, v) - G_1(p)], \quad (30)$$

$$v^{k+1} = v^k + \Delta t \sum_{l=0}^{n_p-1} \alpha_l [F_2(u, v) - G_2(p)], \quad (31)$$

where $k = t/\Delta t$ represents the time steps and the coefficients n_p and α_l define a specific method: $n_p = 1$, $\alpha_0 = 1$ (first-order forward Euler); $n_p = 2$, $\alpha_0 = \frac{3}{2}$, $\alpha_1 = -\frac{1}{2}$ (second-order Adams–Bashforth); and $n_p = 3$, $\alpha_0 = \frac{23}{12}$, $\alpha_1 = -\frac{4}{3}$, $\alpha_2 = \frac{5}{12}$ (third-order Adams–Bashforth).

4. THE CORRECTED PRESSURE EQUATION

Gresho and Sani [1] derived an equation for pressure in such a way that for $\nabla \cdot \mathbf{u}_0 = 0$, the system given by Equations (1) and (2) can be replaced by

$$\frac{\partial \mathbf{u}}{\partial t} + \mathbf{u} \cdot \nabla \mathbf{u} + \nabla p = \frac{1}{Re} \nabla^2 \mathbf{u}, \quad (32)$$

$$\nabla^2 p = \nabla \cdot \left(\frac{1}{Re} \nabla^2 \mathbf{u} - \mathbf{u} \cdot \nabla \mathbf{u} \right), \quad (33)$$

where the boundary condition for p is given by

$$\mathbf{n} \cdot \nabla p = \frac{\partial p}{\partial n} = \frac{1}{Re} \nabla^2 u_n - \left(\frac{\partial u_n}{\partial t} + \mathbf{u} \cdot \nabla u_n \right) \quad \text{for } t \geq 0. \quad (34)$$

The discretization of the pressure equation, being a derived one, requires special care in order to control the accumulation of numerical errors that might invalidate the continuity equation. This means there is a need to introduce corrective terms into the pressure equation.

Consider the momentum equations discretized as

$$\mathbf{u}_{i,j}^{k+1} = \mathbf{u}_{i,j}^k + \Delta t \sum_{l=0}^{n_p-1} \alpha_l [\mathbf{F}(\mathbf{u}_{i,j}^{k-l}) - \nabla p_{i,j}^{k-l}], \tag{35}$$

where n_p and α_l depend upon the employed Adams–Bashforth method, $\mathbf{F}(\mathbf{u}^k)$ being the discretization operator of the convective and diffusive terms.

Applying the divergence operator to both sides of (35) results in

$$\nabla \cdot \mathbf{u}_{i,j}^{k+1} = \nabla \cdot \mathbf{u}_{i,j}^k + \Delta t \sum_{l=0}^{n_p-1} \alpha_l [\nabla \cdot \mathbf{F}(\mathbf{u}_{i,j}^{k-l}) - \nabla^2 p_{i,j}^{k-l}]. \tag{36}$$

The incompressibility condition at the $(k + 1)$ th time step, $\nabla \cdot \mathbf{u}^{k+1} = 0$, is then characterized by

$$\nabla^2 p_{i,j}^k = \nabla \cdot \mathbf{F}(\mathbf{u}_{i,j}^{k-l}) + \frac{\nabla \cdot \mathbf{u}_{i,j}^{k+1}}{\alpha_0 \Delta t} + \frac{1}{\alpha_0} \sum_{l=0}^{n_p-1} \alpha_l [\nabla \cdot \mathbf{F}(\mathbf{u}_{i,j}^{k-l}) - \nabla^2 p_{i,j}^{k-l}]. \tag{37}$$

It is observed that, for the Euler method, the above correction coincides with the dilatation term $D_i = \nabla \cdot \mathbf{u}^n / \Delta t$ [7–9].

Equation (37) can be written in the compact form

$$\nabla^2 p^k = \nabla \cdot \mathbf{H}(\mathbf{u}^k), \tag{38}$$

where

$$\mathbf{H}(\mathbf{u}^k) = \mathbf{F}(\mathbf{u}^k) + \frac{\mathbf{u}^k}{\alpha_0 \Delta t} + \frac{1}{\alpha_0} \sum_{l=0}^{n_p-1} \alpha_l [\mathbf{F}(\mathbf{u}^{k-l}) - \nabla p^{k-l}]. \tag{39}$$

Now, the Laplacian of the pressure is discretized with second-order central differences on a staggered grid

$$\nabla^2 p_{i,j} \approx \frac{p_{i-1,j} + p_{i,j-1} - 4p_{i,j} + p_{i+1,j} + p_{i,j+1}}{h^2}, \tag{40}$$

where $h = \Delta x = \Delta y$. Thus, Equation (38) becomes

$$p_{i-1,j} + p_{i,j-1} - 4p_{i,j} + p_{i+1,j} + p_{i,j+1} = h(H_{1_{i+1,j}} - H_{1_{i,j}} + H_{2_{i,j}} - H_{2_{i,j}}), \tag{41}$$

where $H_{1_{i,j}}$ and $H_{2_{i,j}}$ are the x and y components of $\mathbf{H}(\mathbf{u})$ respectively, applied at the points $(i\Delta x, (j + \frac{1}{2})\Delta y)$ for the first component and $((i + \frac{1}{2})\Delta x, j\Delta y)$ for the second one.

For good convergence of the discretized Poisson equation with a Neumann condition, the compatibility relationship (15) must hold exactly on the discretized domain, i.e. [10,16]

$$\sum_{i,j \in \Omega} \nabla^2 p_{i,j} = \sum_{i,j \in \Gamma} \frac{\partial p_{i,j}}{\partial \eta}. \tag{42}$$

By adding (41) for all points of the square domain, you have

$$\begin{aligned} & \sum_{i=1}^{n-1} \sum_{j=1}^{m-1} p_{i-1,j} + p_{i,j-1} - 4p_{i,j} + p_{i+1,j} + p_{i,j+1} \\ & = h \sum_{i=1}^{n-1} \sum_{j=1}^{m-1} H_{1_{i+1,j}} - H_{1_{i,j}} + H_{2_{i,j+1}} - H_{2_{i,j}}, \end{aligned} \tag{43}$$

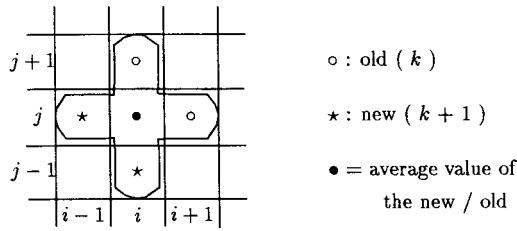


Figure 2. Pressure molecule.

with

$$S_1 = \begin{bmatrix} -2 & 1 & & & & \\ 1 & -3 & 1 & & & \\ & & \ddots & \ddots & \ddots & \\ & & & 1 & -3 & 1 \\ & & & & 1 & -2 \end{bmatrix}_{n \times n}, \quad S_2 = \begin{bmatrix} -3 & 1 & & & & \\ 1 & -4 & 1 & & & \\ & & \ddots & \ddots & \ddots & \\ & & & 1 & -4 & 1 \\ & & & & 1 & -3 \end{bmatrix}_{n \times n}$$

and I is the identity matrix of order n .

At time $k = 0$, the vector \mathbf{p}^0 contains the values of the pressure at interior points, i.e.

$$\mathbf{p}^0 = [p_{1,1}^0 \ p_{2,1}^0 \cdots p_{n,1}^0 \ p_{1,2}^0 \cdots p_{2,2}^0 \cdots p_{n,2}^0 \cdots p_{1,m}^0 \ p_{2,m}^0 \cdots p_{n,m}^0]^T.$$

The vector \mathbf{b} contains all values $n_{i,j}^0, v_{i,j}^0$ from the right-hand-side of (45)–(48), which are given initial values, and this has the particular form

$$\mathbf{b} = [0 \cdots 0 \ b_{mn-n+1} \ 0 \cdots 0 \ b_{mn}]_{m \times n}^T,$$

where

$$b_{mn-n+1} = \frac{2\nu}{h} \quad \text{and} \quad b_{mn} = -\frac{2\nu}{h}.$$

Hence, \mathbf{b} is a non-zero vector.

The above singular system can be solved by several methods: least-squares, iterative or LU [25,22,21].

5.2. The one-step pressure updating

Once the pressure is initialized, the interior pressure values $p_{i,j}$ at time $t + \Delta t$ are computed with the following one-step and explicit scheme (Figure 2):

$$p_{i,j}^{k+1} = \frac{1}{4} [p_{i-1,j}^{k+1} + p_{i,j-1}^{k+1} + p_{i+1,j}^k + p_{i,j+1}^k] - \frac{h^2}{4} \nabla \cdot \mathbf{H}(\mathbf{u}_{i,j}^{k+1}), \tag{51}$$

which incorporates by simple averaging, old and new values for the pressure.

This updating of the pressure field can be written in matrix terms as

$$B\mathbf{p}^{k+1} + C\mathbf{p}^k = -\mathbf{Q}(\mathbf{u}^{k+1}), \tag{52}$$

where

5.4. Extension to three-dimensional domains

The case of a three-dimensional cubic cavity can be easily handled. For a velocity field $\mathbf{u} = (u, v, w)$ on a staggered grid, consider

$$\begin{aligned} u_{i_x, i_y, i_z} &= u(i_x \Delta x, (i_y + \frac{1}{2}) \Delta y, (i_z + \frac{1}{2}) \Delta z), \\ v_{i_x, i_y, i_z} &= v((i_x + \frac{1}{2}) \Delta x, i_y \Delta y, (i_z + \frac{1}{2}) \Delta z), \\ w_{i_x, i_y, i_z} &= w((i_x + \frac{1}{2}) \Delta x, (i_y + \frac{1}{2}) \Delta y, i_z \Delta z), \\ p_{i_x, i_y, i_z} &= p((i_x + \frac{1}{2}) \Delta x, (i_y + \frac{1}{2}) \Delta y, (i_z + \frac{1}{2}) \Delta z). \end{aligned}$$

The discretized momentum equations read

$$\mathbf{u}_{i_x, i_y, i_z}^{k+1} = \mathbf{u}_{i_x, i_y, i_z}^k + \Delta t \sum_{l=0}^{n_p-1} \alpha_l [\mathbf{F}(\mathbf{u}_{i_x, i_y, i_z}^{k-l}) - \nabla p_{i_x, i_y, i_z}^{k-l}], \tag{53}$$

where the operator \mathbf{F} has a similar meaning to that in the two-dimensional case.

The equation for the pressure, including correcting terms, becomes

$$\nabla^2 p_{i_x, i_y, i_z}^k = \nabla \cdot \mathbf{F}(\mathbf{u}_{i_x, i_y, i_z}^k) + \frac{\nabla \cdot \mathbf{u}_{i_x, i_y, i_z}^k}{\alpha_0 \Delta t} + \frac{1}{\alpha_0} \sum_{l=0}^{n_p-1} \alpha_l [\nabla \cdot \mathbf{F}(\mathbf{u}_{i_x, i_y, i_z}^{k-l}) - \nabla^2 p_{i_x, i_y, i_z}^{k-l}]. \tag{54}$$

The discretization of the Laplacian operator on a cubic cavity by second-order central differences and the fulfillment of the discrete compatibility relationship lead to the one-step and explicit scheme

$$\begin{aligned} p_{i_x, i_y, i_z}^{k+1} &= \frac{1}{6} [p_{i_x-1, i_y, i_z}^{k+1} + p_{i_x+1, i_y, i_z}^{k+1} + p_{i_x, i_y-1, i_z}^{k+1} + p_{i_x, i_y+1, i_z}^{k+1} + p_{i_x, i_y, i_z-1}^{k+1} + p_{i_x, i_y, i_z+1}^{k+1}] \\ &\quad - \frac{h^2}{6} \nabla \cdot \mathbf{H}(\mathbf{u}_{i_x, i_y, i_z}^k), \end{aligned} \tag{55}$$

where

$$\mathbf{H}(\mathbf{u}^k) = \mathbf{F}(\mathbf{u}^k) + \frac{\mathbf{u}^k}{\alpha_0 \Delta t} + \frac{1}{\alpha_0} \sum_{l=1}^{n_p-1} \alpha_l [\mathbf{F}(\mathbf{u}^{k-l}) - \nabla p^{k-l}]. \tag{56}$$

Here $h = \Delta x = \Delta y = \Delta z$.

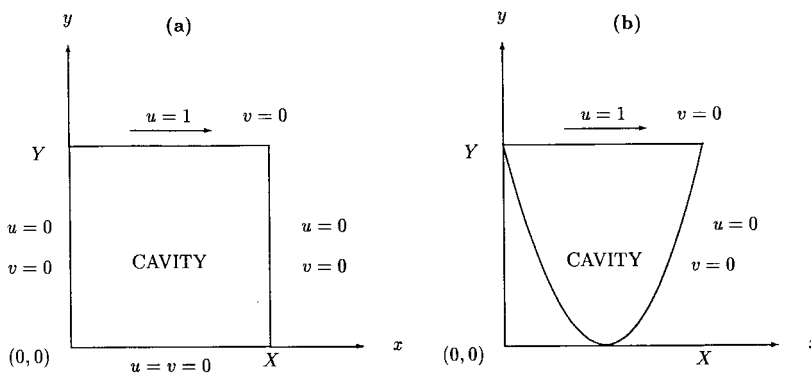


Figure 3. Driven cavity flow: (a) rectangular; (b) curved.

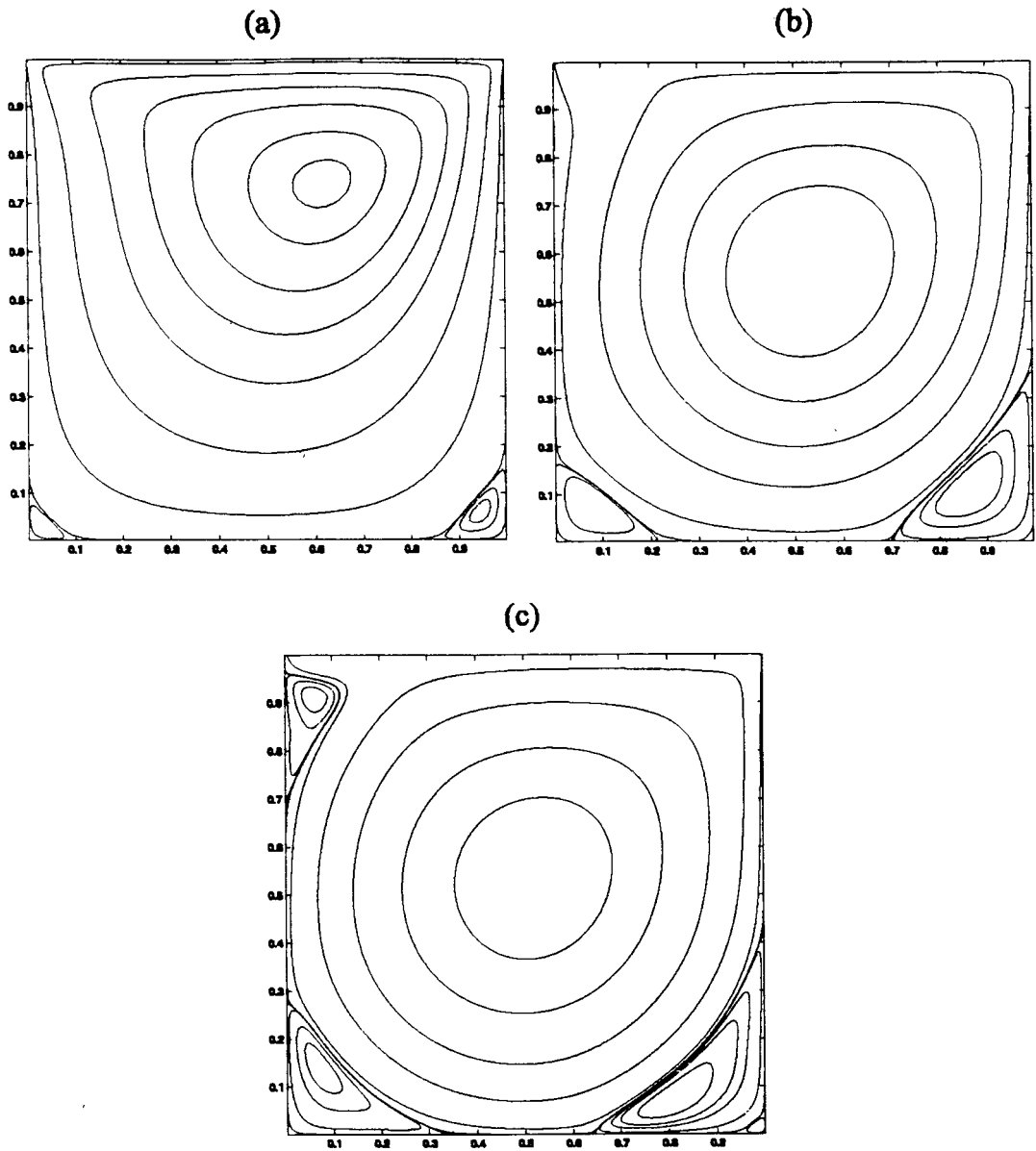


Figure 4. Streamlines: (a) $Re = 100$; (b) $Re = 1000$; (c) $Re = 5000$.

6. NUMERICAL SIMULATIONS

Consider the incompressible viscous flow within a cavity that is induced by the shear movement of the upper wall, with uniform horizontal velocity $u_T = 1$, and keeping fixed the other walls. The driven cavity flow is often employed for testing and comparing numerical techniques for solving the Navier–Stokes equations [2,11–13,24] (Figure 3).

The horizontal velocity boundary conditions are

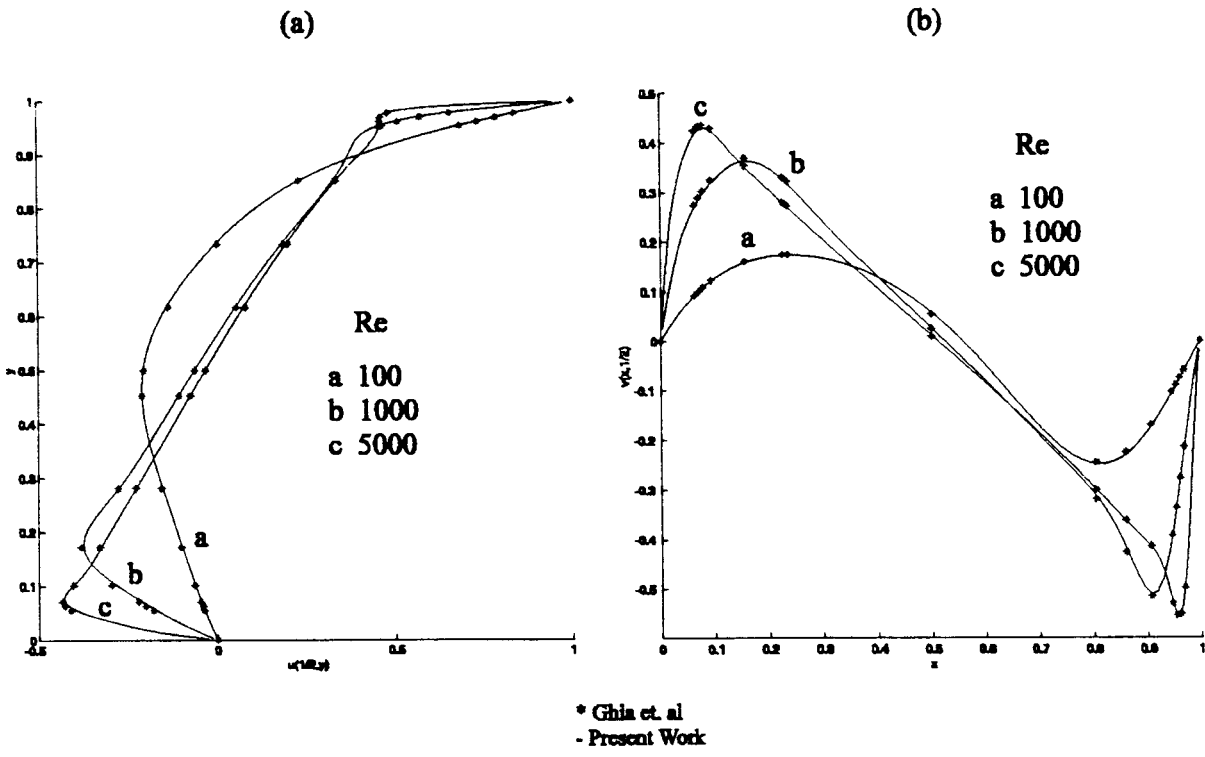


Figure 5. Velocity profiles: (a) $x = 0.5$; (b) $y = 0.5$.

$$u(x, 0, t) = v(0, y, t) = v(X, y, t) = 0, \quad u(x, Y, t) = u_T = 1,$$

and the normal velocity conditions are

$$u(0, y, t) = u(X, y, t) = v(x, 0, t) = v(x, Y, t) = 0,$$

where X and Y are the linear dimensions of the cavity. It shall be assumed that at time $t_0 = 0$ the velocity field is zero.

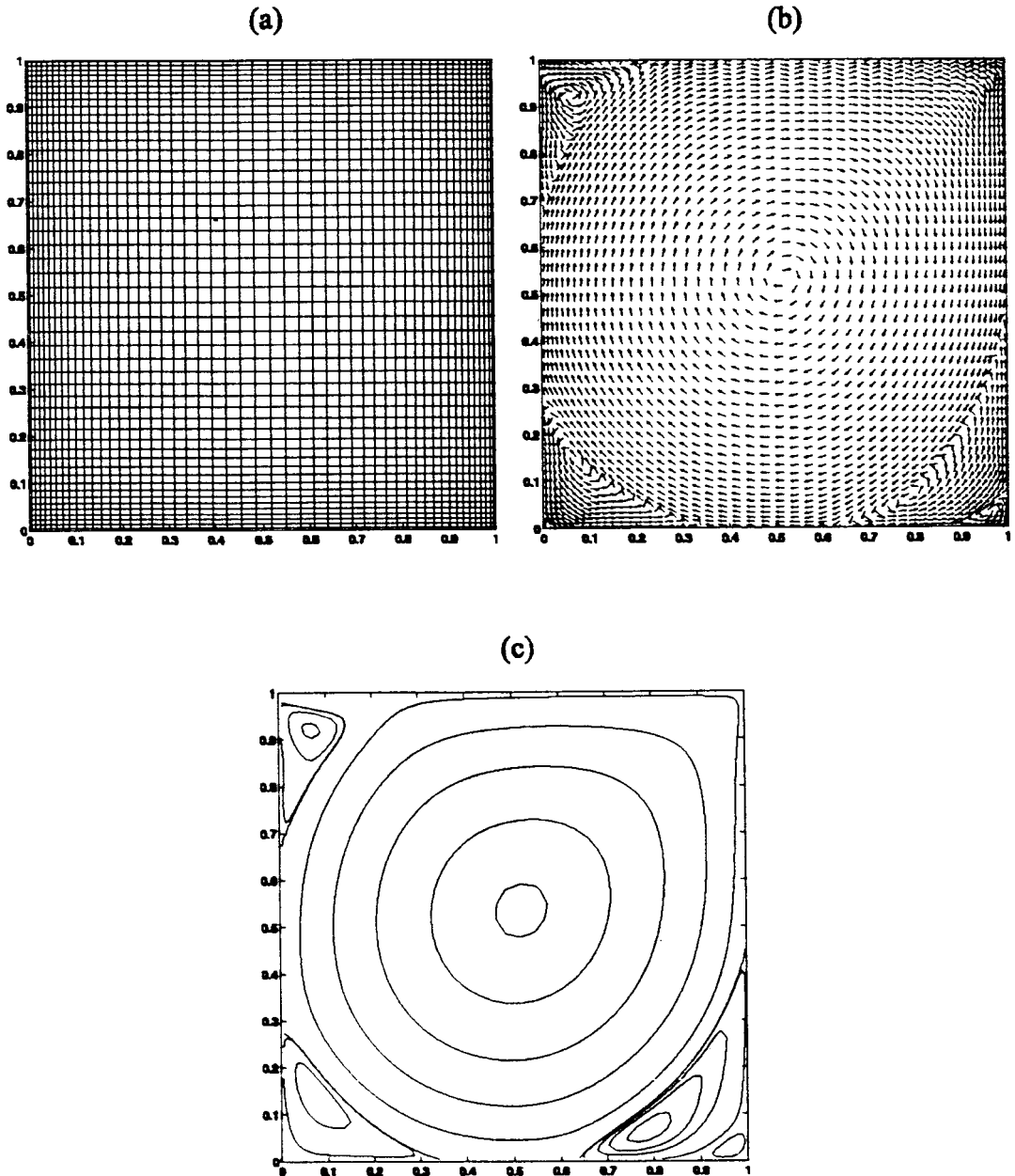


Figure 6. Non-uniform grid: (a) grid 50×50 ; (b) normalized velocity field; (c) streamlines.

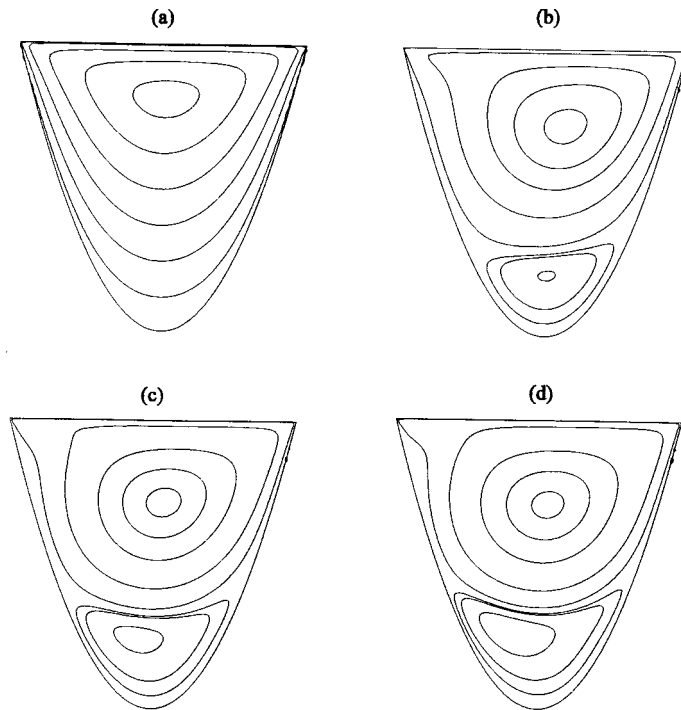


Figure 7. Curved cavity: (a) $Re = 10$; (b) $Re = 400$; (c) $Re = 1000$; (d) $Re = 2000$.

The governing equations were considered in non-dimensional form for

$$\bar{x} = \frac{x}{X}, \quad \bar{y} = \frac{y}{X}, \quad \bar{u} = \frac{u}{u_T}, \quad \bar{v} = \frac{v}{u_T}, \quad \bar{t} = \frac{tu_T}{X}, \quad \bar{p} = \frac{p}{\rho u_T^2}, \quad Re = \frac{u_T X}{\nu}.$$

The simulations were performed for $Re = 100$, 1000 and 5000 and compared with the results of Ghia *et al.* [4]. Figure 4 shows the streamlines and the appearance of the primary vortex, the secondary and tertiary vortices at the lower and upper left corners of the cavity. Figure 5 shows the velocity profiles at the centerlines of the cavity ($y = 0.5$ and $x = 0.5$) compared with those of Ghia *et al.* [4]. For $Re = 100$ and 1000 , it was enough to consider a 66×66 non-uniform grid, refined at the walls, while for $Re = 5000$, a 130×130 refined grid was considered. However, good results can be obtained with smaller refined grids. Figure 6 shows the flow for $Re = 7000$ with a refined grid of 50×50 .

The proposed algorithm was derived, for simplicity, with a rectangular domain. However, it works too with more complex geometries, as shown by the simulations made for a curved cavity. Figure 7 exhibits the results for a parabolic bottom with $Re = 10$, 400 , 1000 and 2000 .

In order to test the non-iterative one-step pressure updating for three-dimensional domains, a cubic cavity was considered. Although the geometry is relatively simple, the flow is quite complex and appropriate for testing computational codes [14].

Figure 8 shows the flow for $Re = 400$ with a grid $60 \times 60 \times 60$. It can be observed from the upper and frontal views that the flow exhibits some kind symmetry, which is to be expected from the boundary conditions. Some authors [15] make use of this observation for reducing the computational time. However, there was no need to such a device in the present computation. The reason being that the aim was to observe if such symmetry could be detected

with the proposed non-iterative pressure algorithm, which does not need to update the pressure in a symmetric way.

The pattern of the streamlines for a cubic cavity is certainly more complex than the two-dimensional case. It can be observed from Figure 9 that the flow moves between the wall and the center of the cavity besides circulating around the axis of the main vortex. Plate 1 illustrates isobaric surfaces. The pressure at the interior of the cavity is near zero and the extreme values are obtained at the upper corners. The negative values of the pressure being at the upper left corner and center of the vortex, while the positive ones occur at the bottom and upper right corner of the cavity.

7. CONCLUSIONS

An algorithm has been developed for the numerical solution of the incompressible Navier–Stokes equations with a central difference scheme in primitive variables and the Neumann boundary condition for the pressure on a staggered grid. The algorithm solves without any iteration a Poisson equation that is transient due to the Neumann condition for the pressure.

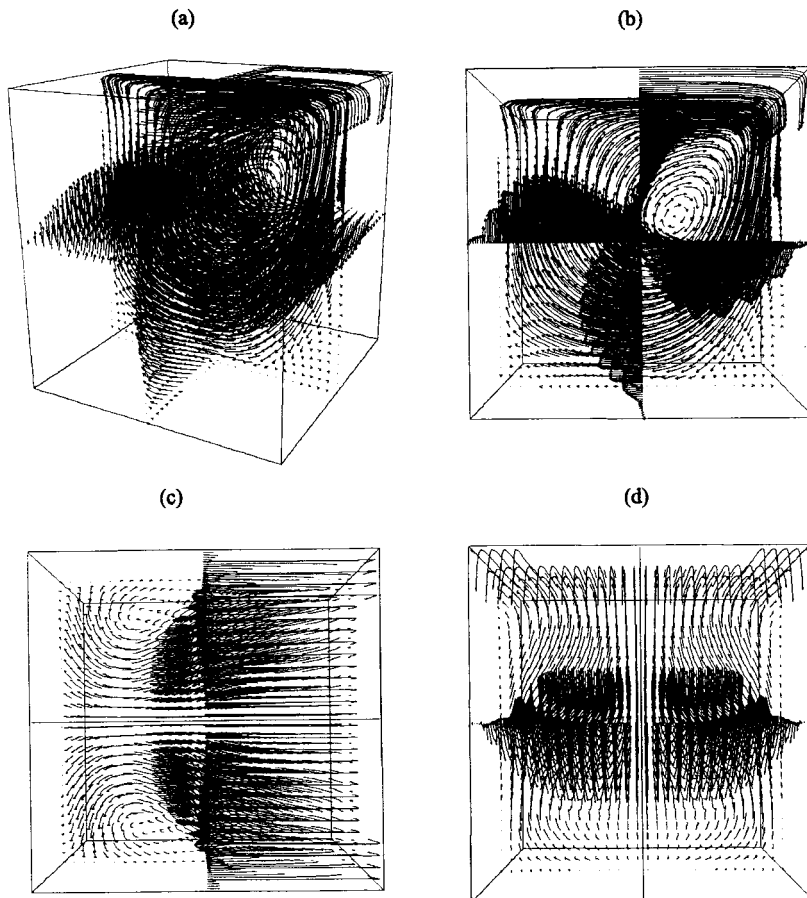


Figure 8. Cubic driven cavity flow at $Re = 400$: (a) perspective; (b) lateral view; (c) upper view; (d) frontal view.

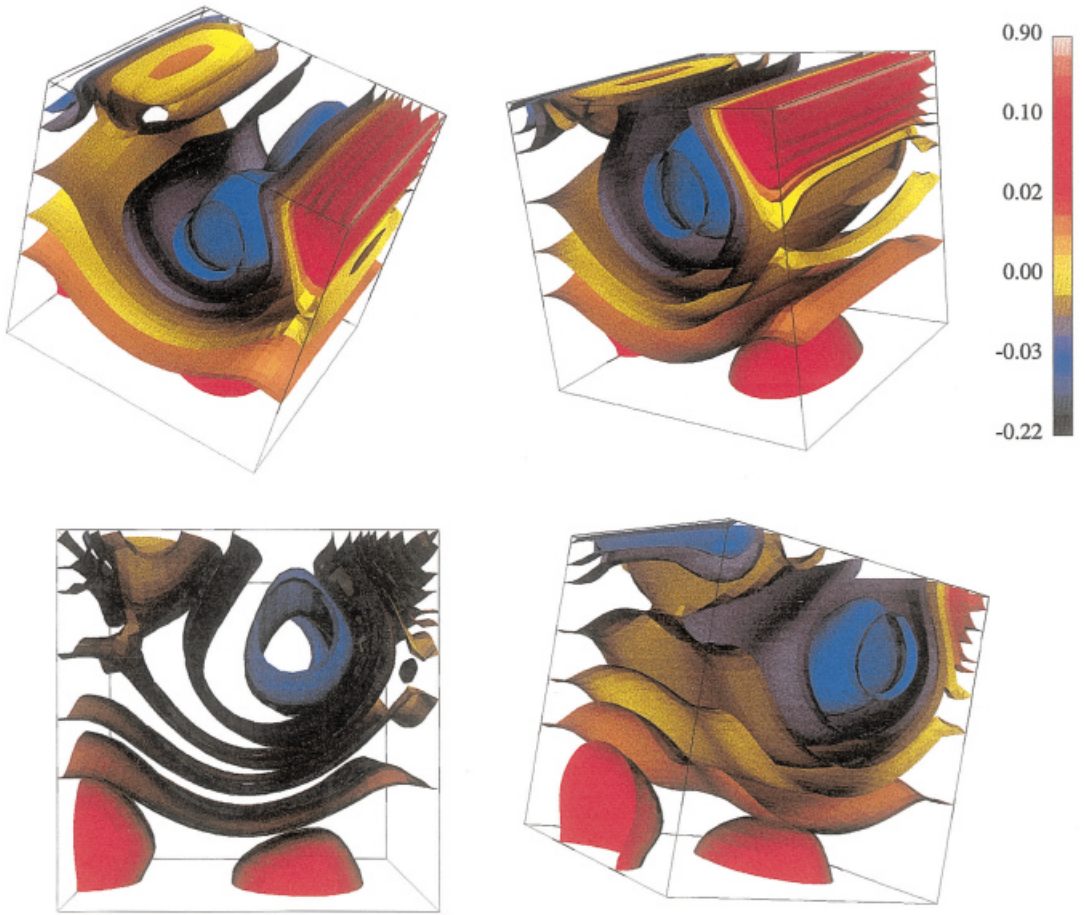


Plate 1. Driven cavity isobaric surfaces at $Re = 400$.

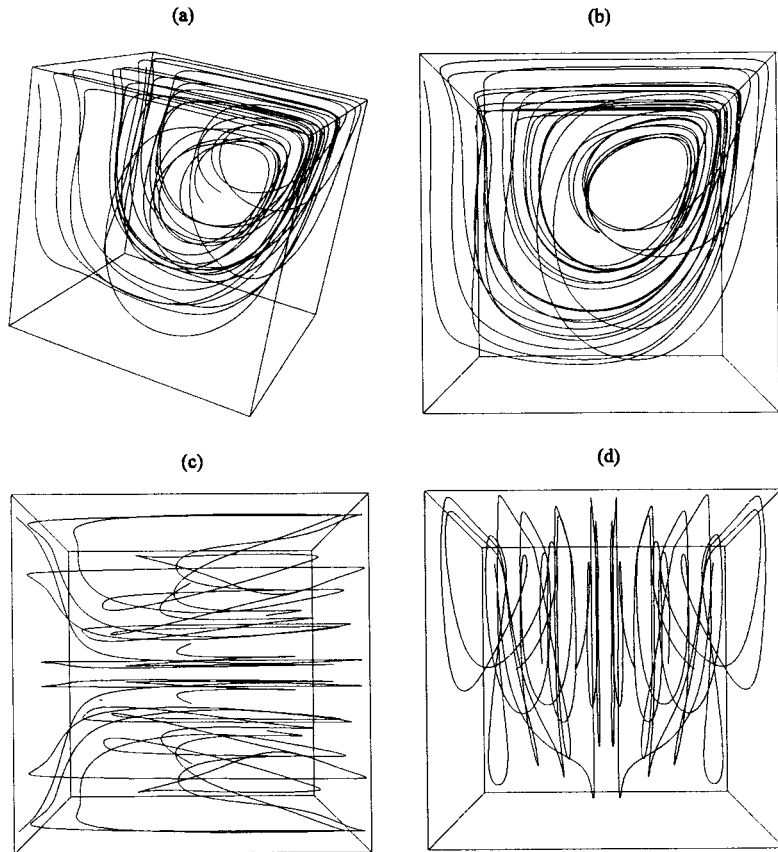


Figure 9. Driven cavity streamlines at $Re > 400$: (a) perspective; (b) lateral view; (c) upper view; (d) frontal view.

This algorithm was tested with the driven cavity flow problem for several Reynolds numbers, uniform and non-uniform grids, curved domains and a three-dimensional cubic cavity. The apartition of the central vortex and the recirculation with secondary and tertiary eddies were observed. As the Reynolds number increases, the central vortex moves toward the geometrical center of the cavity as shown before by Burggraf [3], Ghia *et al.* [4] and Schreiber and Keller [5].

The matrix formulation allows the influence of the Neumann conditions to be followed for the pressure when integrating the velocity and pressure fields at interior points. A correction of the pressure equation was introduced, and for increasing the time step and to diminish the number of iterations, other time integration methods can be used.

The formulation of the current algorithm follows the unified operator approach introduced by Casulli [2], which allows the consideration of, with minor modifications, the upwind and semi-Lagrangian methods.

Numerical simulations were carried out for a broad range of Reynolds numbers. The results were compared with the existing solutions [4] showing a very good agreement. Besides this, simulations done for the cubic and parabolic cavities illustrating that the algorithm can handle three-dimensional and non-rectangular domains.

REFERENCES

1. P.M. Gresho and R.L. Sani, 'On pressure boundary conditions for the incompressible Navier–Stokes equations', *Int. J. Numer. Methods Fluids*, **7**, 1111–1145 (1987).
2. V. Casulli, 'Eulerian–Lagrangian Methods for the Navier–Stokes equations at high Reynolds number', *Int. J. Numer. Methods Fluids*, **8**, 1349–1360 (1988).
3. O.R. Burggraf, 'Analytical and numerical studies of the structure of steady separated flows', *J. Fluid Mech.*, **24**, 113–151 (1966).
4. U. Ghia, K.N. Ghia and C.T. Shin, 'High-*Re* solutions for incompressible flow using the Navier–Stokes equations and a multigrid method', *J. Comput. Phys.*, **48**, 387–411 (1982).
5. R. Schreiber and H.B. Keller, 'Driven cavity flows by efficient numerical techniques', *J. Comput. Phys.*, **49**, 310–333 (1983).
6. R. Temam, *Navier–Stokes Equations*, 3rd. edn., North-Holland, Amsterdam, 1985.
7. W.F. Ames, *Numerical Methods for Partial Differential Equations*, 3rd edn., Academic Press, San Diego, 1992.
8. J.H. Ferziger and M. Perić, *Computational Methods for Fluid Dynamics*, Springer, Berlin, 1996.
9. P.J. Roache, *Computational Fluid Dynamic*, Hermosa, Albuquerque, NM, 1982.
10. S. Abdallah, 'Numerical solutions for the pressure Poisson equation with Neumann boundary conditions using a non-staggered grid, I', *J. Comput. Phys.*, **70**, 182–192 (1987).
11. A.T. Degani and G.C. Fox, 'Parallel multigrid computation of the unsteady incompressible Navier–stokes equations', *J. Comput. Phys.*, **128**, 223–236 (1996).
12. M.M. Gupta, 'High accuracy solutions of incompressible Navier–Stokes equations', *J. Comput. Phys.*, **93**, 343–359 (1991).
13. S. Hou, Q. Zou, S. Chen, G. Doolen and A.C. Cogley, 'Simulation of flow by the lattice Boltzmann method', *J. Comput. Phys.*, **118**, 329–347 (1995).
14. W.T. Wang and T.H. Sheu, 'An element-by-element BIGGSTAB iterative method for three-dimensional steady Navier–Stokes equations', *J. Comput. Appl. Math.*, **79**, 147–165 (1997).
15. X.H. Wu, J.Z. Wu and J.M. Wu, 'Effective vorticity–velocity formulations for three-dimensional incompressible viscous flows', *J. Comput. Phys.*, **122**, 68–82 (1995).
16. B.J. Alfrink, 'On the Neumann problem for the pressure in a Navier–Stokes model', *Proc. 2nd Int. Conf. on Numerical Methods in Laminar and Turbulent Flow*, Venice, 1981, pp. 389–399.
17. E. Bravo and J.R. Claeysen, 'Simulação central pare escoamento incompressível em variáveis primitivas e condições de Neumann para a pressão', *XIX Cong. Nacional de Matemática Aplicada e Computacional-CNMAC*, Goiânia, Brasil, 1996.
18. K.E. Brenam, S.L. Campbell, and L.R. Petzold, *Numerical Solution of Initial Value Problems in Differential–Algebraic Equations*, Elsevier Science Publishing, New York, 1989.
19. A. Castro, and Bravo, 'Upwind simulation of an incompressible flow with natural pressure boundary condition on a staggered grid', *SIAM Annual Meeting*, Kansas City, USA, 1996.
20. V. Casulli, 'Eulerian–Lagrangian methods for hyperbolic and convection dominated parabolic problems', in C. Taylor, D.R.J. Owen and E. Hinton (eds.), *Computational Methods for Non-Linear Problems*, Pineridge Press, Swansea, 1987, pp. 239–269.
21. J.R. Claeysen and H.F. Campos Velho, 'Initialization using non-modal matrix for a limited area model', *Boletim SBMAC*, **4**, 41–48 (1994).
22. B.N. Datta, *Numerical Linear Algebra and Applications*, Brooks/Cole Publishing Company, Monterey, CA, 1995.
23. F.H. Harlow and J.E. Welsh, 'Numerical calculation of time dependent viscous incompressible flow with free surface', *Phys. Fluids*, **8**, 2182–2189 (1965).
24. G. Mansell, J. Walter and E. Marschal, 'Liquid–liquid driven cavity flow', *J. Comput. Phys.*, **110**, 274–284 (1994).
25. C.R. Rao S.K. Mitra, *Generalized Inverse of Matrices and its Applications*, Wiley, New York, 1971.